ACS APPLIED MATERIALS & INTERFACES

Research Article

Cite This: ACS Appl. Mater. Interfaces 2019, 11, 14702−14712

www.acsami.org

Wettability Control of Co−SiO_2@Ti−Si Core−Shell Catalyst to Enhance the Oxidation Activity with the In Situ Generated Hydroperoxide

Meng Liu,[†,‡] Song Shi,[*,†] Li Zhao,[†,‡] Min Wang,[§] Guozhi Zhu,[†,‡] Jin Gao,[†] and Jie Xu[*,†]

[†]State Key Laboratory of Catalysis, Dalian National Laboratory for Clean Energy, Dalian Institute of Chemical Physics, Chinese Academy of Sciences, Dalian 116023, People's Republic of China

[‡]University of Chinese Academy of Sciences, Beijing 100049, People's Republic of China

[§]Zhang Dayu School of Chemistry, Dalian University of Technology, Dalian 116024, People's Republic of China

Supporting Information

ABSTRACT: With the aim of utilizing O_2 as an oxidant, cascade reaction strategy was usually employed by first transforming O_2 into the in situ generated hydroperoxide and then oxidized the substrate. To combine the two steps more efficiently to get a higher reaction rate, a series of core−shell catalysts with core and shell having different wettabilities were designed. The catalysts were characterized by transmission electron microscopy, UV−vis spectroscopy, Fourier transform infrared, sessile water contact angle, among other methods. These catalysts were applied in the research of the diphenyl sulfide oxidation by the in situ generated hydroperoxide derived from ethylbenzene oxidation. Through control experiments, the hydrophobic modification in the shell and core will influence different steps of the overall cascade reaction. Further insight into the reaction illustrated that the overall reaction rate was not simply an adduct of the promotion effects from the two steps, which was mainly attributed to the inhibition effect for the co-oxidation of ethylbenzene with diphenyl sulfide. Through the guidance of the relationship, a rationally designed core−shell catalyst with appropriate modifying organic groups showed an enhanced performance of the overall cascade reaction. The rational design of the catalysts would provide a reference for other cascade reactions.

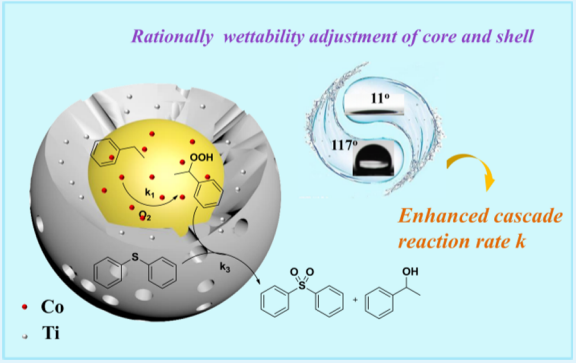

KEYWORDS: *core−shell, cascade reaction, wettability adjustment, in situ generated hydroperoxide, aerobic oxidation*

1. INTRODUCTION

Selective oxidation of the organic compounds with dioxygen was a green and sustainable process but also challenging[1−3] due to the inert nature of dioxygen. Recently, cascade reactions involving several consecutive reactions have attracted much attention owing to the advantages of efficient atom economy, simplified reaction procedures, decreased waste, etc.[4−11] To utilize O_2 as an oxidant, cascade reaction strategy was developed by first transforming O_2 into the in situ generated hydroperoxide, which then oxidized the substrate. Through the cascade strategy, olefins,[12−16] hydrocarbon,[17] sulfide,[18−20] and phenol[21] all have been successfully oxidized by O_2 by combining different catalysts. In addition, this strategy has also been involved in the industrial production of propene oxide through in situ generated cumyl hydroperoxide or 1-phenylethyl hydroperoxide (PEHP).[22,23]

The cascade process with the in situ generated hydroperoxide typically contained two main steps: the generation of hydroperoxide and the oxidation of the substrate with hydroperoxide. The hydroperoxide played a key role in the process, as it connected the two steps. However, the properties of the hydroperoxide were quite special: it was unstable and easily self-decomposed or catalytically decomposed;[24−27] furthermore, besides the oxidant for the second step, the hydroperoxide also served as radical initiator for the first step (hydrocarbon oxidation) to generate hydroperoxide. The above-mentioned properties made this cascade process unique and resulted in two main challenges, which limited the further improvement of this process: (1) The active and unstable property would lead to the poor utilization of the in situ generated hydroperoxide, meaning that much of the generated hydroperoxide did not participate in the second step. (2) The dual roles of the hydroperoxide as an oxidant and an initiator had multiple influences in the two steps. The overconsumption of the hydroperoxide would decrease the radical initiation in the first step, resulting in the decrease of the hydroperoxide content. Therefore, the balance of the two steps based on the insight of the relationship between them is another key factor

Received: November 9, 2018
Accepted: April 4, 2019
Published: April 4, 2019

DOI: 10.1021/acsami.8b19704
ACS Appl. Mater. Interfaces 2019, 11, 14702−14712

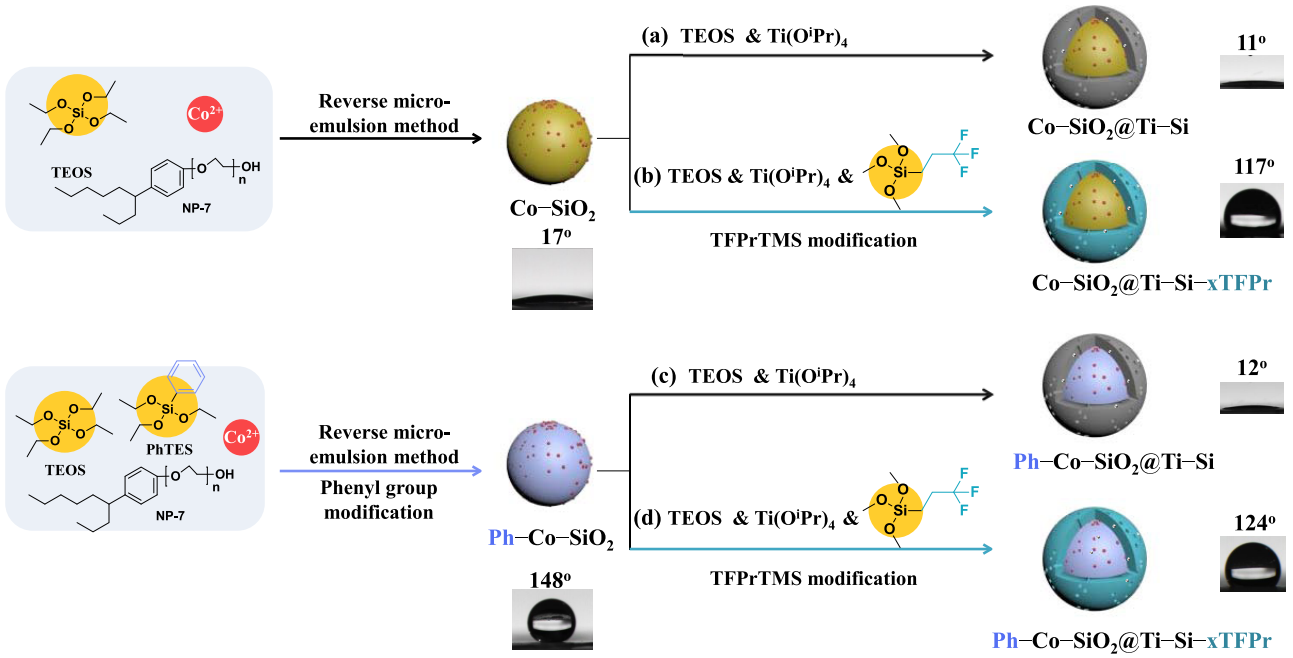

Figure 1. Procedures to adjust the wettability of the core–shell catalysts.

to enhance the total reaction rate. In our previous work, a core–shell combination strategy was developed to design the catalyst, realizing the high utilization efficiency of in situ generated PEHP through the spatial tightly combined catalyst sites.[28] However, the balance and insight into the relationship between the two steps remained a challenge.

Special designed catalysts were necessary to separately adjust the two steps of the reaction and finally get insight into the relationship of the steps. To guarantee the effective utilization of hydroperoxide, core–shell combination strategy was preserved. Besides the core–shell structure, the state of the support was significant for catalyst performance, which would influence the properties of the active sites, for example, the electronic state, size, morphology, etc. Among various important properties of the support, wettability, which can directly affect the adsorption and desorption of the reactant and the product, was noteworthy.[29−32] Therefore, wettability plays a key role in the catalytic performance.[33−38] Several groups including ours have reported that adjustable wettability could affect the catalytic performances of the kind of reactions,[39−42] which made it a good candidate to adjust for the catalyst. Therefore, controlling the wettability of the inner core and the outer shell of the core–shell catalyst for the cascade aerobic oxidation is a promising way to enhance the catalytic activity, but it is also a challenging task and has been rarely explored.

Herein, based on previous work, we designed and synthesized various core–shell catalysts with the core and shell having different wettabilities to research the balance of the two steps (Figure 1). These catalysts were applied in the cascade oxidation of diphenyl sulfide by in situ generated PEHP derived from ethylbenzene oxidation (Scheme 1). We focused on the effect toward the reaction of the different hydrophobic modification on the shell and the core separately. The effect on each individual step of the cascade reaction and the overall cascade reaction were carefully studied. It was found that the overall cascade reaction rate was not the simple adduct of the individual steps. A deep insight into the relationship between the individual steps and the overall reaction was gained and a rationally designed core–shell catalyst with high activity was prepared.

Scheme 1. Raction Pathway of the Cascade Reaction

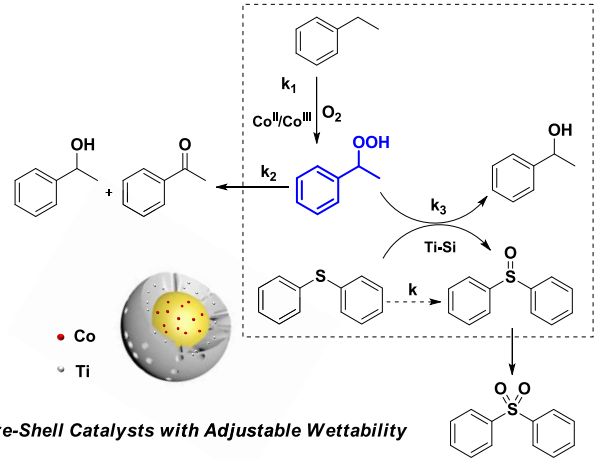

2. EXPERIMENTAL SECTION

2.1. Chemicals and Materials. Tetraethyl orthosilicate, cetyltrimethyl ammonium bromide (CTAB), ethylbenzene, and $NH_3{\cdot}H_2O$ (28%) were bought from Tianjin Kermel Chemical Reagent Co., Ltd. Acetylacetone and cobalt(II) acetate tetrahydrate were obtained from Sinopharm Chemical Reagent Co., Ltd. Triethoxphenylsilane (PhTES), trimethoxymethylsilane (MeTMS), and poly(oxyethylene) nonylphenol ether (NP-7) were bought from Aladdin Chemicals (Shanghai, China). Titanium(IV) isopropoxide and fluorotriethoxysilane were purchased from Alfa Aesar. Trimethoxy(3,3,3-trifluoropropyl)silane (TFPrTMS) was purchased from TCI. Trimethoxy(propyl)silane (PrTMS) was obtained from Adamas.

2.2. Catalyst Preparation. Synthesis of the core ($Co–SiO_2$ and $Ph–Co–SiO_2$):[39] Three solutions were mixed for the synthesis of $Co–SiO_2$. Solution A: 8 g of *n*-butyl alcohol, 32 g of cyclohexane, and 15 g of NP-7; solution B: 60 mg of cobalt(II) acetate tetrahydrate, 5.5 g of H_2O, and 2.1 g of $NH_3{\cdot}H_2O$; solution C: 25 mmol of

DOI: 10.1021/acsami.8b19704
ACS Appl. Mater. Interfaces 2019, 11, 14702−14712

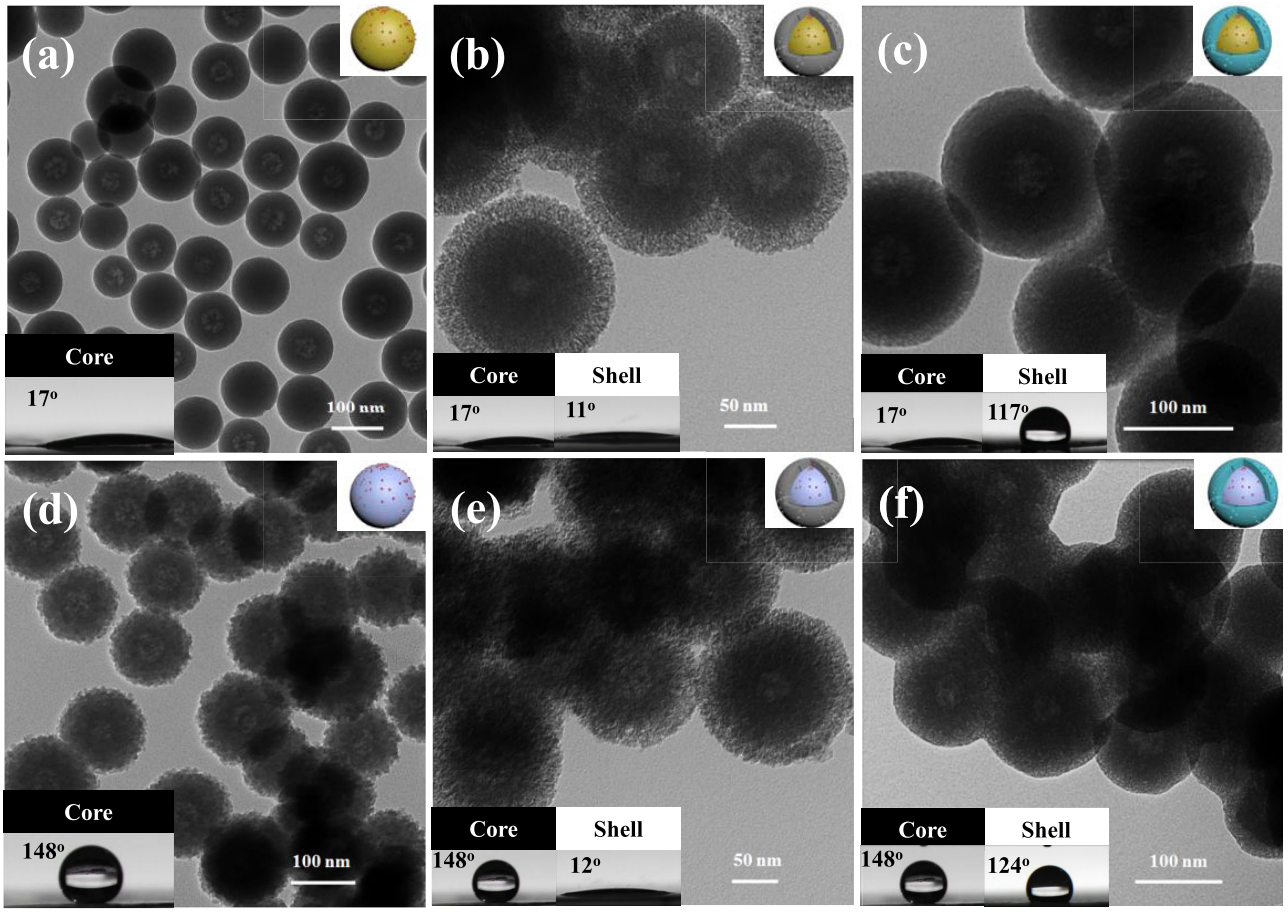

Figure 2. TEM images of the catalysts (a) Co−SiO_2, (b) Co−SiO_2@Ti−Si, (c) Co−SiO_2@Ti−Si−35TFPr, (d) Ph−Co−SiO_2, (e) Ph−Co−SiO_2@Ti−Si, and (f) Ph−Co−SiO_2@Ti−Si−35TFPr (the insets on the left corner are the water droplets of relative materials).

tetraethoxysilane (TEOS). First, weighed solution A in a 250 mL bottle, stirred for 10 min, then mixed and added solution B, stirred for 40 min, and solution C was added dropwise with stirring. As for Ph−Co−SiO_2, solution C was composed of TEOS (21.25 mmol) and PhTES (3.75 mmol), with other procedures kept the same as for Co−SiO_2. Ten milliliters of ethanol was added in the bottle after stirring for 12 h; the material was separated through centrifugation, washed with refluxed ethanol, and dried in an oven at 80 °C.

Synthesis of Co−SiO_2@Ti−Si: 0.5 g of Co−SiO_2 was dispersed in a 1 L bottle, which contains ethanol (150 mL) and H_2O (200 mL). Sonicated the mixture for 20 min, CTAB (0.75 g) and $NH_3{\cdot}H_2O$ (2.90 mL) were added in and stirred for 20 min. Then, 8 mg of titanium(IV) isopropoxide, 7 mg of acetylacetone, and 0.70 g of TEOS were blended and added in slowly. After 12 h, the mixture was centrifuged to separate the material. The template of CTAB was removed by washing with NH_4NO_3/ethanol (6 g/L) at 65 °C each time for 30 min, and the procedure was repeated three times. Then, the mixture was further washed with ethanol and H_2O and finally dried at 80 °C.

Synthesis of shell-modified core−shell catalysts (Co−SiO_2@Ti−Si-*x*TFPr, the *x* represents the mole percentage of the added TFPrTMS in the total silica amount of the shell part, which varied as 5, 15, 25, and 35%): For the shell formation procedure, except that TFPrTMS replaced partial TEOS (the adding amount is supplied in Table S8), other procedures were the same as for Co−SiO_2@Ti−Si. Synthesis of Ph−Co−SiO_2@Ti−Si: The Ph−Co−SiO_2 was used instead of Co−SiO_2, whereas other procedures were the same as for Co−SiO_2@Ti−Si. The amount of titanium(IV) isopropoxide and acetylacetone added were 30 and 28 mg for Ph−Co−SiO_2@4Ti−Si, respectively.

Synthesis of core−shell-modified catalysts: Ph−Co−SiO_2 was used instead of Co−SiO_2, whereas other procedures were the same as for Co−SiO_2@Ti−Si−*x*TFPr. Synthesis of modified shells: The shell followed the same procedures as the core−shell catalysts except the addition of core.

PEHP synthesis:[28] PEHP was separated from the mixtures of ethylbenzene auto-oxidation reaction at 130 °C with dioxygen. The NaOH aqueous solution was added to extract PEHP, and the aqueous phase was collected. Then, $NaHCO_3$ was added with plenty of *n*-hexane, and retained the organic phase after complete mixing. After the extraction of acetonitrile from *n*-hexane, acetonitrile solution with PEHP was obtained.

2.3. Catalytic Reactions. The aerobic oxidation reactions were all carried out in a sealed autoclave reactor with 1.0 MPa of O_2. In a typical ethylbenzene oxidation, 4 mL of ethylbenzene, 6 mL of acetonitrile, and 50 mg of catalyst were added in, and the mixture kept at 120 °C for the desired time.

The cascade oxidation of diphenyl sulfide (ethylbenzene co-oxidation with diphenyl sulfide) was conducted as follows: 1 mmol of diphenyl sulfide, 4 mL of ethylbenzene, 6 mL of acetonitrile, and 50 mg of catalyst were added. Afterward, the reactor was heated to 120 °C.

Diphenyl sulfide oxidation with PEHP and the PEHP decomposition reactions were conducted under nitrogen in Ace Glass pressure tubes. The substrates were added and the tubes replaced with N_2 if possible. In addition, the conversion versus time profiles in Figure 9d were performed in a sealed autoclave reactor.

2.4. Product Analysis. Analysis of the reaction was through Agilent 6890N gas chromatography with a HP-INNOWAX column (30 m × 0.320 mm). Quantification of the reactants and products relied on an internal standard method with an internal standard compound of *p*-dichlorobenzene. The concentration of PEHP was determined by a titration method, which first used PEHP to oxidize

DOI: 10.1021/acsami.8b19704
ACS Appl. Mater. Interfaces 2019, 11, 14702−14712

excess amount of KI to obtain I_2, and the obtained I_2 was titrated by $Na_2S_2O_3$ standard solution. PEHP was calculated from the consumption amount of $Na_2S_2O_3$.

2.5. Catalyst Characterization. The transmission electron microscopy (TEM) images were obtained from a HITACHI HT7700. Quantachrome Autosorb-1 and Quadrasorb SI were used to carry out the N_2 adsorption−desorption experiments at 77 K. The diffuse reflectance spectroscopy (DRS) UV−vis spectra were tested on a Shimadzu UV-2600. Fourier transform infrared (FT-IR) spectra were acquired on a Bruker Tensor 27 instrument with the testing range of 4000−400 cm^{-1} in the KBr media. X-ray photoelectron spectrum (XPS) was collected on a ThermoESCALAB 250Xi. PerkinElmer ICP-OES 7300DV instrument was used to analyze inductively coupled plasma (ICP) results. The contact angle measuring system JC 2000 C1 was used to detect the water contact angels with a 5 μL water droplet.

3. RESULTS AND DISCUSSION

3.1. Composition and Properties of the Catalysts. *3.1.1. Cores with Adjustable Wettability.* The procedures to synthesize the core−shell catalysts with different wettabilities are illustrated in Figure 1. As elucidated, the core of the core−shell catalysts was synthesized through a reverse-phase microemulsion method. During the synthetic process, when TEOS was the only silica source, the obtained material was Co−SiO_2, which acted as the hydrophilic core. Applying PhTES instead of partial TEOS, a phenyl group modified Ph−Co−SiO_2 was attained, which acted as the hydrophobic core. Through sessile water droplet contact angle measurements, a water contact angle (WCA) of 17° (Figure 2a) was obtained for Co−SiO_2, suggesting its hydrophilic property. However, the WCA of Ph−Co−SiO_2 was 148° (Figure 2d), demonstrating the hydrophobic nature of Ph−Co−SiO_2; in addition, the difference of the wettability of the two cores was due to the introduction of phenyl group in the cobalt nanocomposites, which was proved in the previous report.[39] The existence of the phenyl group was proved by FT-IR spectroscopy. In the spectrum of Ph−Co−SiO_2 in Figure 3b, the peaks at 742 and 699 cm^{-1} were attributed to the monosubstituted phenyl group.[43] To clarify the morphologies, the transmission electron microscopy (TEM) was conducted; a uniform sphere for Co−SiO_2, whereas a fluffy appearance for Ph−Co−SiO_2 were attributed to the volume effect of the phenyl group (Figure 2a,d). As shown in Table 1, the analysis of the N_2 sorption isotherms (Figure S1) gave the values of S_{BET} of 61 and 269 m^2/g for Co−SiO_2 and Ph−Co−SiO_2, respectively. The increased S_{BET} for Ph−Co−SiO_2 was due to its fluffy appearance.

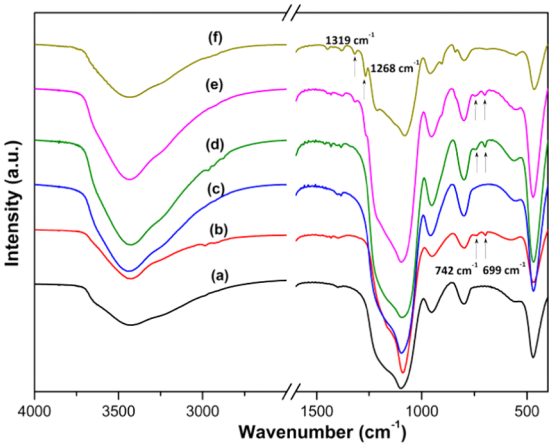

Figure 3. FT-IR spectra of (a) Co−SiO_2, (b) Ph−Co−SiO_2, (c) Co−SiO_2@Ti−Si, (d) Ph−Co−SiO_2@ Ti−Si, (e) Ph−Co−SiO_2@Ti−Si-15TFPr, and (f) Ti−Si−15TFPr.

3.1.2. Core−Shell Catalyst with Hydrophilic Core and Hydrophilic Shell. The hydrophilic core−shell catalyst was prepared on the basis of Co−SiO_2, and the formation of the shell was through a process involving the structure-directing agent of CTAB, the silica source of TEOS, and the Ti source of $Ti(OiPr)_4$.[28,44] The WCA of Co−SiO_2@Ti−Si was 11° (Figure 2b), indicating its hydrophilic property. Besides, from the TEM image in Figure 2b, a core−shell structure and a permeable shell were confirmed. Furthermore, the porous properties of Co−SiO_2@Ti−Si proved the formation of a porous shell. As shown in Table 1, S_{BET} of 498 m^2/g showed an obvious increase over Co−SiO_2 (61 m^2/g). The pore size of Co−SiO_2@Ti−Si was 3.2 nm, as calculated by the NLDFT method, indicating a mesoporous shell was generated on Co−SiO_2.

3.1.3. Core−Shell Catalyst with Hydrophilic Core and Hydrophobic Shell. As Figure 1b shows, different from Co−SiO_2@Ti−Si, TFPrTMS replaced partial TEOS participating in the co-condensation on Co−SiO_2 to form the TFPr group modified hydrophobic shell of Co−SiO_2@Ti−Si−xTFPr. Furthermore, the WCA of the Co−SiO_2@Ti−Si−35TFPr was 117° (Figure 2c), which showed hydrophobic properties. Compared with the 11° of Co−SiO_2@Ti−Si, the introduction of the TFPr group was proved, along with the successful transformation of the wettability of the core−shell catalysts. From Figure 2c, after modification, the core−shell structure was still maintained. The existence of the TFPr group was confirmed by FT-IR spectroscopy; the relative result is shown in Figure 3f. As Ti−Si−15TFPr was characterized by its increased content of the TFPr group, followed by comparison with Ti−Si, the peaks at 1319 and 1268 cm^{-1} of Ti−Si−15TFPr evidenced the existence of the TFPr group.[39]

3.1.4. Core−Shell Catalyst with Hydrophobic Core and Hydrophilic Shell. When the hydrophobic Ph−Co−SiO_2 was the core, Ph−Co−SiO_2@Ti−Si was synthesized (Figure 1c). The WCA of Ph−Co−SiO_2@Ti−Si was 12° (Figure 2e), compared with 148° for Ph−Co−SiO_2; the obvious decrease of the WCA indicated the transformation of hydrophobic to hydrophilic property. Then, the structure of Ph−Co−SiO_2@Ti−Si was studied; in Figure 2e, the core−shell structure was directly observed. However, due to the shell formation, the roughness of the core was not easy to notice. To this point, the peaks of the monosubstituted phenyl group were observed from the FT-IR spectrum (Figure 3d), indicating the phenyl group was still present after the shell formation. The mesoporous characteristic of the shell was investigated with the isotherm shown in Figure S1. The increase of S_{BET} from 269 to 479 m^2/g further confirmed the formation of the shell on the fluffy core. While, the increase of S_{BET} for Ph−Co−SiO_2@Ti−Si was inferior to the Co−SiO_2@Ti−Si when comparing with their relative cores, which was due to the core differences.

3.1.5. Core−Shell Catalyst with Hydrophobic Core and Hydrophobic Shell. As illustrated in Figure 1d, the core−shell catalysts of Ph−Co−SiO_2@Ti−Si−xTFPr was synthesized with Ph−Co−SiO_2 as the core and the TFPr group modified hydrophobic Ti−Si as the shell. The WCA of Ph−Co−SiO_2@Ti−Si−35TFPr was 124° (Figure 2f), indicating the achievement of the core−shell catalyst wettability adjustment. The

DOI: 10.1021/acsami.8b19704
ACS Appl. Mater. Interfaces 2019, 11, 14702−14712

Table 1. Textual Properties of the As-Synthesized Catalysts

catalysts	ICP AES		S_{BET} (m^2/g)[a]	V_p (cm^3/g)	D_p (nm)[b]
	Co (wt %)	Ti (wt %)			
Co−SiO_2	1.11		61	0.14	
Ph−Co−SiO_2	1.31		269	0.29	
Co−SiO_2@Ti−Si	0.74	0.23	498	0.49	3.2
Co−SiO_2@Ti−Si-5TFPr	0.73	0.22	433	0.47	3.5
Ph−Co−SiO_2@Ti−Si	0.84	0.22	479	0.48	2.8
Ph−Co−SiO_2@Ti−Si-5TFPr	0.75	0.23	503	0.40	2.8
Ph−Co−SiO_2@Ti−Si-15TFPr	0.72	0.20	521	0.38	2.6

[a]The surface area was determined by Brunauer−Emmett−Teller (BET) method. [b]D_p was calculated by non-local density functional theory (NLDFT) method.

reservation of the phenyl group in the core and the successful introduction of the TFPr group in the shell were concluded from the FT-IR results in Figure 3e. And, the core−shell structure of Ph−Co−SiO_2@Ti−Si−*x*TFPr was confirmed through the TEM results (Figures 2f and S3), with a shell formed on the core. In addition, through the N_2 adsorption−desorption analysis, the mesoporous shells were confirmed (Table 1).

UV−vis DRS was utilized to analyze the coordination state of Ti; the spectra are shown in Figure 4. The maximum

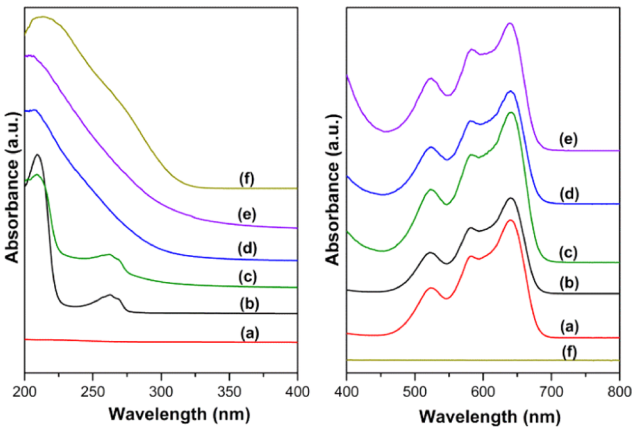

Figure 4. UV−vis DRS spectra of the catalysts (a) Co−SiO_2, (b) Ph−Co−SiO_2, (c) Ph−Co−SiO_2@Ti−Si, (d) Co−SiO_2@Ti−Si, (e) Co−SiO_2@Ti−Si−5TFPr, and (f) Ti−Si−15TFPr.

absorption peaks of the materials are at around 210 nm, which showed that Ti existed mainly as an isolated tetrahedral Ti(IV).[45−48] However, the peaks of phenyl groups were also positioned at 210 and 260 nm, which would overlap the information of Ti in the catalysts, such as Ph−Co−SiO_2 and Ph−Co−SiO_2@Ti−Si (Figure 4b,c). To verify if the Ti coordination state would be affected by the hydrophobic Ph−Co−SiO_2 core, a catalyst denoted as Ph−Co−SiO_2@4Ti−Si with four times the Ti content compared to the materials here was analyzed by X-ray photoelectron spectroscopy (XPS). In Figure 5, the deconvolution peak of the Ti 2p spectrum located at a binding energy of 459.2 eV was for Ti $2p_{3/2}$, and the extra framework Ti(IV) is 457.8 ± 0.2 eV; in general, the higher binding energy was attributed to Ti(IV) in a tetrahedral coordination.[49,50] Hence, Ti in the synthesized catalysts would be mainly in a tetrahedral coordination. In addition, the three consecutive peaks positioned at 450−750 nm were typical for Co(II) in a tetrahedral environment.[51,52] The as-synthesized catalysts showed no noticeable differences in this aspect.

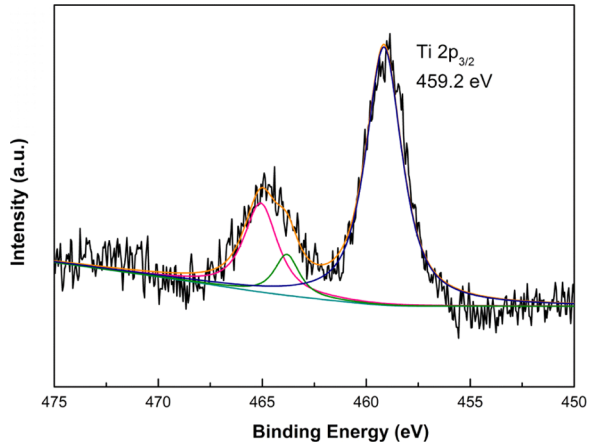

Figure 5. Ti 2p XPS spectrum of the catalyst Ph−Co−SiO_2@4Ti−Si.

3.2. Oxidation of Diphenyl Sulfide with Dioxygen.

The as-synthesized catalysts were evaluated in the cascade oxidation of diphenyl sulfide with in situ generated PEHP from ethylbenzene oxidation (Scheme 1). The results are exhibited in Table 2. From the reaction results, the core−shell catalysts all performed better than the blank and the single-core catalytic systems (entries 2 and 3). This phenomenon was attributed to the core−shell structure, which could attain a high utilization efficiency of PEHP as our previous work reported.[28] For the core−shell catalysts, when the shell was modified with 5%

Table 2. Cascade Oxidation of Diphenyl Sulfide[a]

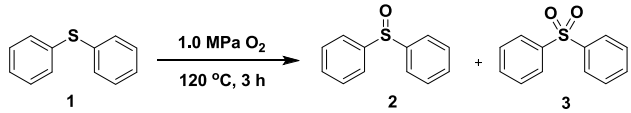

entry	catalyst	conv. (%)	product distribution (%)	
			2	3
1	blank	36	95	5
2	Co−SiO_2	42	95	5
3	Ph−Co−SiO_2	51	97	3
4	Co−SiO_2@Ti−Si	76	65	35
5	Co−SiO_2@Ti−Si-5TFPr	89	50	50
6	Ph−Co−SiO_2@Ti−Si	95	46	54
7	Ph−Co−SiO_2@Ti−Si-5TFPr	98	43	57
8	Ph−Co−SiO_2@Ti−Si-15TFPr	87	61	39

[a]Reaction conditions: 1 mmol of substrate, 4 mL of ethylbenzene, 6 mL of CH_3CN, 50 mg of catalyst.

DOI: 10.1021/acsami.8b19704
ACS Appl. Mater. Interfaces 2019, 11, 14702−14712

molar ratio of TFPr groups, a promoted reaction conversion (89%, Table 2, entry 5) was obtained comparing with the unmodified Co−SiO_2@Ti−Si (76%, Table 2, entry 4), which demonstrated that the hydrophobic environment of the Ti species in the shell could accelerate the oxidation of diphenyl sulfide under the current system. In addition, for the hydrophobic modification of the core by the catalyst Ph−Co−SiO_2@ Ti−Si (entry 6), a 95% conversion was achieved, which implied that the hydrophobic modification of the Co species in the core could also promote total reaction. Combing the hydrophobic modification of the core and shell, Ph−Co−SiO_2@Ti−Si−5TFPr with hydrophobic modification of both the core and shell was synthesized; a conversion of 98% was achieved, which showed a slight increase over Ph−Co−SiO_2@Ti−Si. As the literature reported, hydrophobic environment of the Ti species would facilitate the oxidation of sulfide via peroxide[41,42] to further increase the overall reaction activity; Ph−Co−SiO_2@Ti−Si−15TFPr with the hydrophobic shell modification with more content of organic groups (15% molar ratio of TFPr group) was synthesized. To our surprise, an unexpected decrease of 87% conversion was achieved, exhibiting a minus effect. To further confirm this point, the kinetic studies of the cascade oxidation of diphenyl sulfide were conducted to investigate the phenomenon. A good linear relationship existed between the linear fit of $\ln(C_t/C_0)$ and the reaction time (Figure S7), which demonstrates pseudo-first-order kinetics. The reaction rates are displayed in Figure 6, an

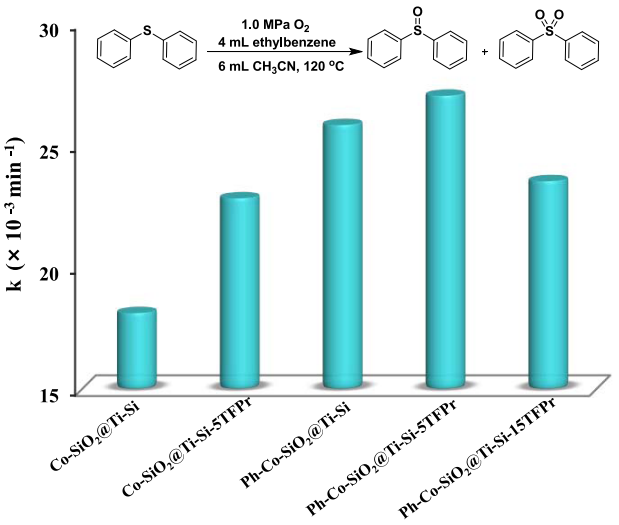

Figure 6. Kinetics study of the cascade oxidation of diphenyl sulfide.

increase of the reaction rate for Co−SiO_2@Ti−Si−5TFPr (22.8×10^{-3} min^{-1}) compared with Co−SiO_2@Ti−Si (18.1×10^{-3} min^{-1}) was observed, which was well in agreement with the batch reaction result. On the other hand, the core-modified Ph−Co−SiO_2@Ti−Si (25.8×10^{-3} min^{-1}) also achieved a better performance than Co−SiO_2@Ti−Si, suggesting the hydrophobic modification of the core was also effective. The above results indicated that appropriate hydrophobic modification individually of the core and shell is effective for the overall reaction performance. However, for the catalyst Ph−Co−SiO_2@Ti−Si−15TFPr with both hydrophobic modification of the core and further hydrophobic modification of the shell, a better performance was expected than the individual modification. Nevertheless, a reaction rate of 23.5×10^{-3} min^{-1} was obtained, which showed a relatively decreased activity than Ph−Co−SiO_2@Ti−Si and Ph−Co−SiO_2@Ti−Si−5TFPr (27.0×10^{-3} min^{-1}) (Figure 6). The unexpected result implied that for the cascade reaction, the overall reaction performance was not simply an adduct of the two consecutive steps. Therefore, investigating the relationships between the whole reaction process and the consecutive steps was necessary for designing efficient core−shell catalysts. The promotion effect of the shell and core modification is discussed below.

3.3. Effect of Hydrophobic Modification of the Shell.

The research on the effect of the hydrophobic modification of the shell was conducted. As mentioned above, different hydrophobic modifications of the shell had different effects on the activities of the cascade reaction. To comprehend the effect of the hydrophobic modification of the shell on the overall reaction in particular, the core−shell catalysts with different hydrophobicities of the shell were synthesized via adjusting the content of the organic groups in the shell, namely, Co−SiO_2@Ti−Si−xTFPr. The core−shell structures of the shell-modified catalysts were confirmed through the TEM images (Figure S3). The as-synthesized catalysts were evaluated in the cascade reaction of diphenyl sulfide oxidation (Figure 7a). Except Co−SiO_2@Ti−Si−5TFPr, which showed the promotion effect, other catalysts with a higher content of the TFPr group all showed decreased conversions than Co−SiO_2@Ti−Si. In addition, the higher the content of TFPr modified, the lower was the conversion achieved. To address this issue, the impacts from the differences of textural property of the catalysts were first ruled out. The catalysts maintained mesoporous shells as the TFPr content increased (Figures S1 and S2). As for the state of the Ti species, the UV−vis DRS spectra of the catalysts are listed in Figure S4, all of which showed a mainly tetrahedral coordination. All these characteristics illustrated the catalysts had little difference except the wettability. The analysis of the reaction process was conducted step by step according to the reaction process. The cascade reaction was divided into mainly three parts, the ethylbenzene oxidation (k_1), the decomposition of PEHP (k_2), and the oxidation of diphenyl sulfide with PEHP (k_3) (Scheme 1). As a primary step of the cascade reaction, ethylbenzene oxidation (k_1) with generating the PEHP which connected the two steps was analyzed. And the PEHP was a key compound in the reaction. The reaction performances of different catalysts for ethylbenzene oxidation represented the ability to generate PEHP, which was the primary chain product of the reaction.[53] The results in Figure 7b indicated quite capable conversions for all the TFPr group modified core−shell catalysts, so did Co−SiO_2@Ti−Si. Furthermore, the differences of the ethylbenzene conversions of Co−SiO_2@Ti−Si−xTFPr were small. This suggested that the decreased performances of Co−SiO_2@Ti−Si−xTFPr (x = 15, 25, 35%) could not be attributed to the oxidation of ethylbenzene. Besides the simple oxidation of ethylbenzene, during the cascade reaction, the oxidation of ethylbenzene proceeded along with oxidation of diphenyl sulfide, which was rendered as the co-oxidation of ethylbenzene. The analysis on the co-oxidation of ethylbenzene is displayed in Figure 7b. A comparison shows that the oxidation of ethylbenzene by all the catalysts had weakened remarkably compared with the oxidation without diphenyl sulfide. An inhibition effect appeared for the co-oxidation of ethylbenzene; furthermore, the inhibition degree enlarged as the content of TFPr increased.

DOI: 10.1021/acsami.8b19704
ACS Appl. Mater. Interfaces 2019, 11, 14702−14712

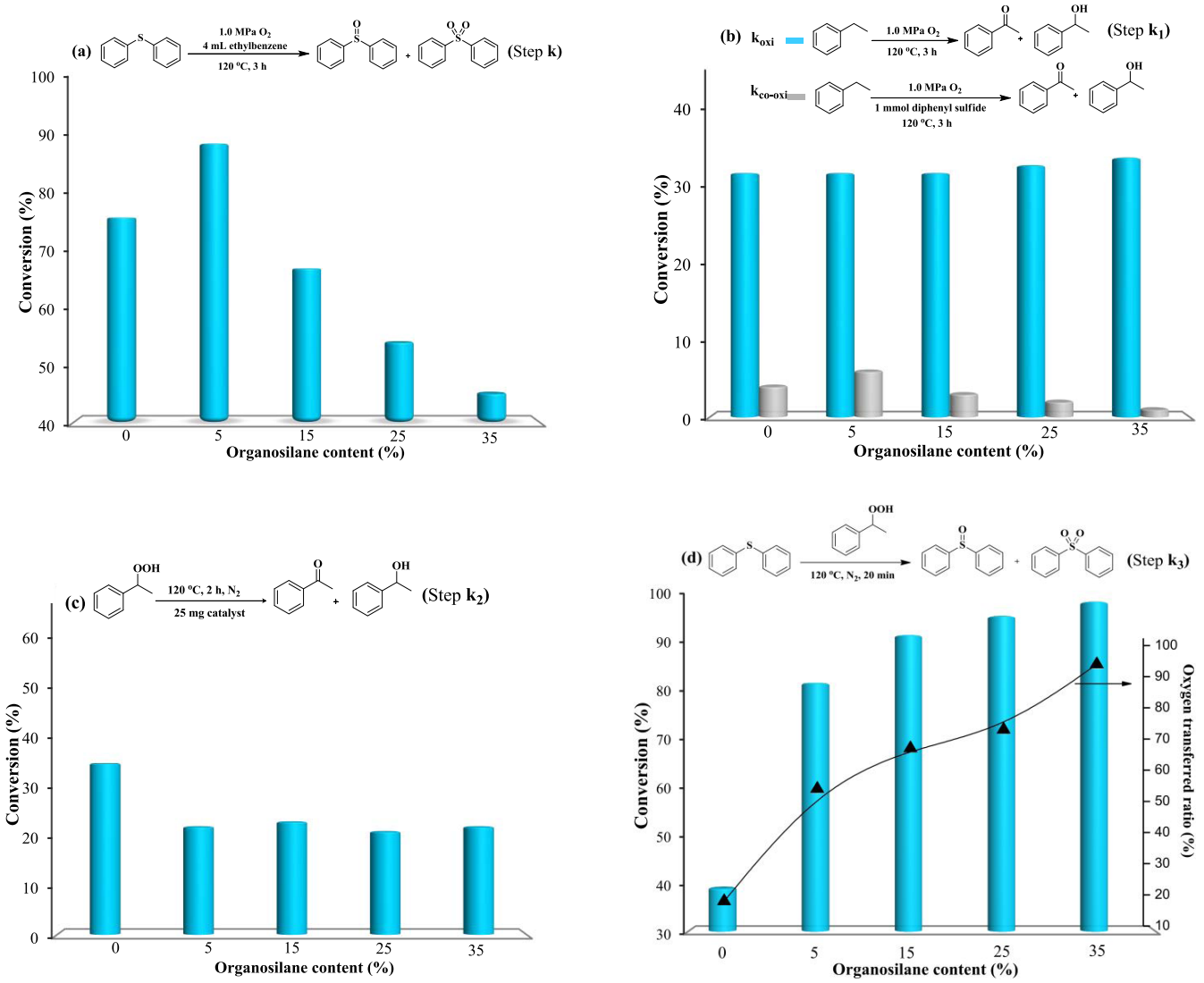

Figure 7. Study on the shell modification effect of Co−SiO_2@Ti−Si−*x*TFPr, (a) diphenyl sulfide aerobic oxidation, (b) ethylbenzene oxidation and co-oxidation, (c) PEHP decomposition, and (d) diphenyl sulfide oxidation with PEHP. (Reactions details are supplied in Tables S3−S6.)

The decomposition of PEHP (k_2) for various contents of TFPr catalysts were also investigated (Figure 7c), with the hydrophobic modified catalysts showing a relatively weaken decomposition activity than Co−SiO_2@Ti−Si; however, for catalysts with various contents of TFPr, the activity remained similar, proving the difference for this step was limited. In addition, the main active site for PEHP decomposition was Co−SiO_2, the Ti−Si showed insufficient conversion of PEHP (Figure S10).

A further exploration was conducted to analyze the effect of diphenyl sulfide oxidation of PEHP (k_3) on the co-oxidation of ethylbenzene through introducing different contents of TFPr group in the shell. The activity of Ti−Si−*x*TFPr was promoted as the content of TFPr group increased, so did the oxygen atom transfer ratio into the generated products from the PEHP (Figure 7d). The promotion results were in accordance with the works reporting that the hydrophobic environment facilitated the sulfide oxidation via peroxide.[41,42] Based on the experimental results, the hydrophobic modification of the shell mainly promoted the sulfide oxidation with PEHP catalyzed by Ti species as expected. However, when the modified catalyst promoted k_3 too much, the performance of the total reaction would be decreased. Since the differences in k_{oxi} and k_2 were limited, the difference in k_3 and $k_{co\text{-}oxi}$ were the key reasons for the differential activity of the shell modification catalysts.

In general, the ethylbenzene oxidation went through a radical mechanism. During the early stage, hydroperoxide was first formed and then decomposed into radicals to initiate the radical chain of hydrocarbon oxidation. A certain concentration of hydroperoxide was needed in the initiation stage. Once the diphenyl sulfide was added, partial PEHP was consumed via the efficient Ti sites (step k_3), which would decrease the concentration of PEHP in the reaction system and slow down the initiation process, resulting various inhibition degrees of step k_1. To further illustrate this issue, the ethylbenzene co-oxidation with various amounts of diphenyl sulfide was conducted. The conversion versus addition amount profile is given in Figure 8. As the addition amount of diphenyl sulfide increased, the inhibition of ethylbenzene oxidation increased, which was due to higher consumption of PEHP. It was further verified by the addition of triphenylphosphine (Ph_3P) in the ethylbenzene oxidation system, which could reduce hydroperoxide to stoichiometric tri-phenylphosphine

DOI: 10.1021/acsami.8b19704
ACS Appl. Mater. Interfaces 2019, 11, 14702−14712

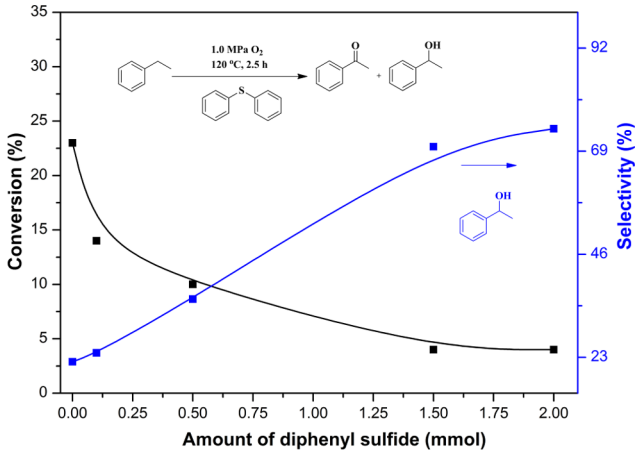

Figure 8. Study on the inhibition effect, conversion of ethylbenzene versus diphenyl sulfide addition amount profile with Co−SiO_2@Ti−Si (standard reaction conditions: 4 mL ethylbenzene, 6 mL CH_3CN, 50 mg of catalyst).

oxide ($POPh_3$) even at room temperature.[54] The control experiment with the addition of Ph_3P showed little conversion (<1%) of ethylbenzene, confirming the inhibition effect being due to the consumption of PEHP (Scheme S1).

Above all, the much increased k_3 cause a decrease in $k_{co\text{-}oxi}$, which, in turn, limited the generation of PEHP. This could explain that excess TFPr group modification in the shell with the promotion effect on the diphenyl sulfide oxidation by PEHP would lead to a low total cascade conversion (Figure 7a). These results implied the appropriate promotion effect of the modified shell was necessary for the overall reaction, which should ensure enough PEHP is generated to ensure diphenyl sulfide oxidation occurred smoothly.

3.4. Effect of Hydrophobic Modification of the Core.

The research on the effect of the hydrophobic modification of the core was investigated. The conversion versus time profiles of the core hydrophilic and hydrophobic catalysts are shown in Figure 9a, which shows that the hydrophobic modification in the core accelerated the cascade oxidation, in line with the above results. The investigation was conducted step by step according to the reaction process.

First, the ethylbenzene oxidation was researched (Figure 9b). As for the oxidation without diphenyl sulfide (k_{oxi}), Ph−Co−SiO_2@Ti−Si (41%) showed an increase of conversion than Co−SiO_2@Ti−Si (32%), which was in accordance with previous works in which the hydrophobic microenvironment of Co−SiO_2 nanocomposite would accelerate the oxidation of ethylbenzene.[39] The co-oxidation of ethylbenzene was also surveyed. The conversion of ethylbenzene co-oxidation was carried out (Figure 9b), and it is worth noticing that there is an obvious decrease of $k_{co\text{-}oxi}$ compared with k_{oxi}, which agreed well with the aforementioned inhibition effect. The core-modified Ph−Co−SiO_2@Ti−Si (10%) showed an advantage of conversion over Co−SiO_2@Ti−Si (4%). The analysis of the above reactions showed that the hydrophobic modification in the core (Co sites) was beneficial for ethylbenzene oxidation in the cascade reaction.

As the formation of PEHP clarified, the utilization of PEHP was analyzed subsequently. According to the results in Figure 9c, Ph−Co−SiO_2@Ti−Si showed a relative fast decomposition rate of PEHP (k_2) than Co−SiO_2@Ti−Si; meanwhile, Ph−Co−SiO_2 also took an advantage over Co−SiO_2. Since the main active site for PEHP decomposition was Co species, it is obvious that the Ph group modified in the core facilitated the decomposition rate. On the other hand, the utilization of PEHP to oxidize diphenyl sulfide (k_3) was evaluated along with the conversion versus time profile shown in Figure 9d. An obvious better reaction performance was observed for Ph−Co−SiO_2@Ti−Si than Co−SiO_2@Ti−Si; to address this issue, the hydrophobic environment of the catalyst also facilitated this step. Based on the experimental results, the hydrophobic modification of the core promoted the three steps during the cascade reactions. According to the above analysis of the shell part, the promotion in k_3 will inhibit the ethylbenzene oxidation, which would lead to a decrease in the total cascade reaction. However, though k_3 was promoted in the core modification, the total reaction was also promoted. This phenomenon was attributed to the ethylbenzene oxidation (k_1), also promoted by the core modification, which could generate far more excess PEHP than consumed. The above analysis demonstrated that the hydrophobic modification in the core would bring fast oxidation of ethylbenzene, which could attain enhanced overall reaction activity.

3.5. Rational Design of the Core−Shell Wettability.

On the basis of the analysis of the core and shell modification, along with the comprehension of the reaction process, the rational combination of the core and shell was necessary to enhance the reaction activity. The promotion effect of hydrophobic modification with the Ph group in the core for the overall reaction was established, whereas the shell modification for the overall reaction needed appropriate promotion effect; combing the two aspects, a rational design of the core−shell catalysts was obtained. For the core modification, according to our previous report,[39] the phenyl and propyl groups (Pr) modified in Co−SiO_2 showed a relatively high activity for ethylbenzene oxidation, whereas the modification of the propyl group achieved a particle size of around 50 nm, which as a core could not form the core−shell structure easily. The Ph group modification was the optimized one. For the shell modification, a survey on the effect of different kinds of organic groups in the shell was conducted; the results are shown in Table S7. The slightly facilitated function was assigned to the propyl group modification, which showed 60% conversion of diphenyl sulfide compared with the nonmodified shell with 48% conversion. The Pr modification would bring a slight promotion effect but less inhibition of ethylbenzene than other organic group modification according to the investigation. The Pr group was chosen as the shell modification group to get an enhanced core−shell catalyst. According to the above analysis, the rationally designed catalyst was Ph−Co−SiO_2@Ti−Si−15Pr. And an enhanced reaction rate (Figure S7) of Ph−Co−SiO_2@Ti−Si−15Pr (28.2×10^{-3} min^{-1}) was achieved with respect to Ph−Co−SiO_2@Ti−Si−15TFPr (23.5×10^{-3} min^{-1}) and Ph−Co−SiO_2@Ti−Si (25.8×10^{-3} min^{-1}).

4. CONCLUSIONS

In summary, a series of multifunctional core−shell catalysts with different wettabilities in the core and shell were designed based on Co−SiO_2@Ti−Si. The wettability of the core and shell could be adjusted separately by precisely modifying organic groups in the core and shell. These catalysts were applied in the research of the diphenyl sulfide oxidation by the in situ generated hydroperoxide to get an enhanced activity. Through control experiments, the hydrophobic modification of

DOI: 10.1021/acsami.8b19704
ACS Appl. Mater. Interfaces 2019, 11, 14702−14712

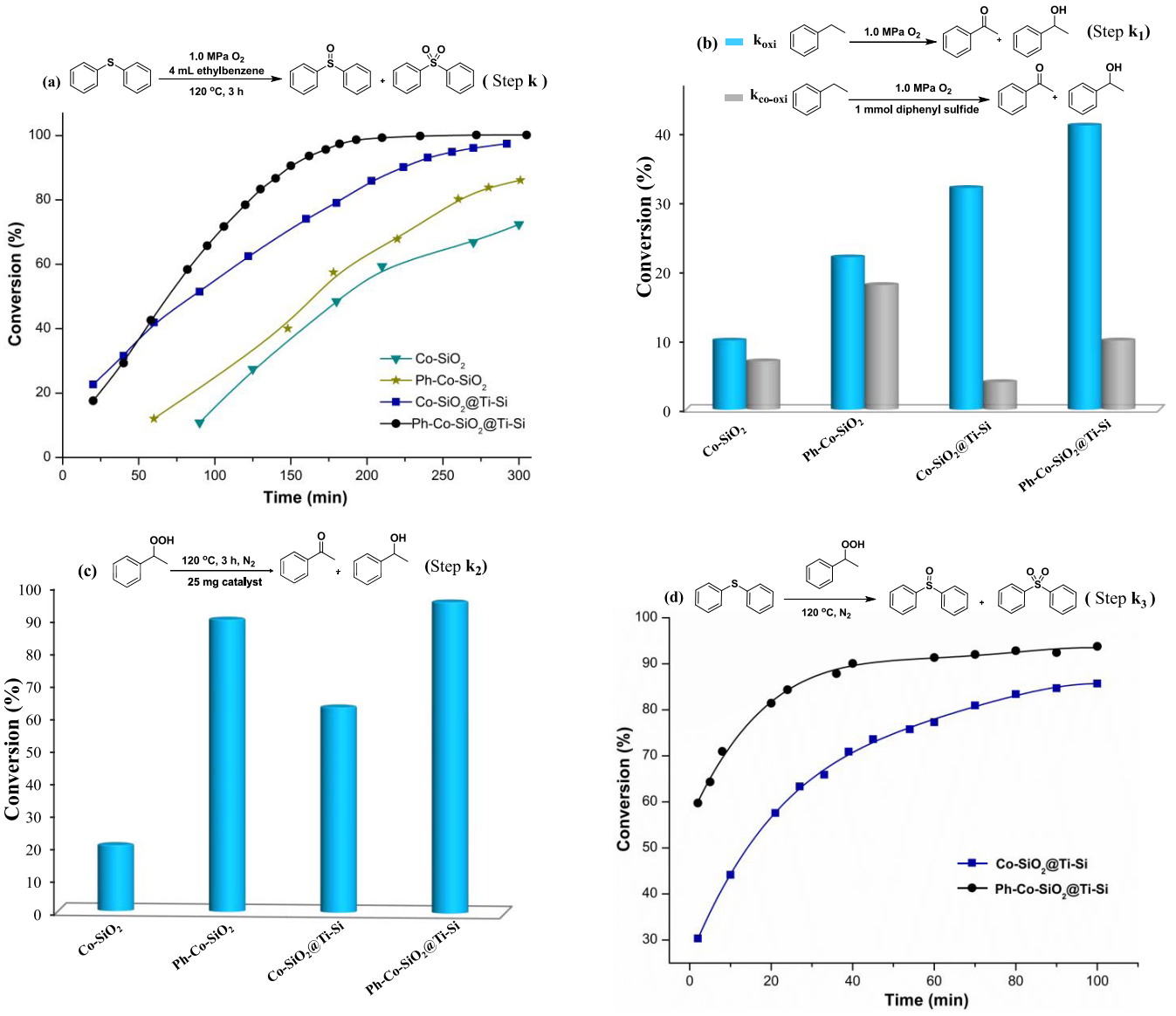

Figure 9. Study on the core modification effect, (a) diphenyl sulfide aerobic oxidation, (b) ethylbenzene oxidation and co-oxidation, (c) PEHP decomposition, and (d) diphenyl sulfide oxidation with PEHP.

the shell mainly promoted the sulfide oxidation by PEHP, whereas the hydrophobic modification of the core promoted all the steps during the cascade reactions. Further investigation illustrated the overall reaction rate was not a simple adduct of individual steps. A much higher reaction rate of the oxidation of diphenyl sulfide by PEHP will hamper the overall reaction rate. Through the guidance of the insight into the relationship, a rationally designed core−shell catalyst with modification of appropriate organic groups was given with an enhanced performance of the overall cascade reaction. The wettability control of the catalysts would provide a reference for catalysts design for the utilization of in situ generated reactions.

■ ASSOCIATED CONTENT

Supporting Information

The Supporting Information is available free of charge on the ACS Publications website at DOI: 10.1021/acsami.8b19704.

Characterization data and relative reaction results; N_2 adsorption−desorption isotherms of the catalysts; TEM images of the modified core−shell catalysts; shell thickness of the core−shell catalysts; diphenyl sulfide oxidation linear fit of $\ln(C_t/C_0)$ against the reaction time; decomposition regularity of PEHP over Ti−Si, the blank and Co−SiO_2 (PDF)

■ AUTHOR INFORMATION

Corresponding Authors

*E-mail: shisong@dicp.ac.cn (S.S.).
*E-mail: xujie@dicp.ac.cn (J.X.).

ORCID

Song Shi: 0000-0002-4306-1933
Min Wang: 0000-0002-9072-8331
Jie Xu: 0000-0003-2535-094X

Notes

The authors declare no competing financial interest.

DOI: 10.1021/acsami.8b19704
ACS Appl. Mater. Interfaces 2019, 11, 14702−14712

■ ACKNOWLEDGMENTS

This work was supported by National Natural Science Foundation of China (Grant Nos. 21790331 and 21603218), the Strategic Priority Research Program of Chinese Academy of Sciences (XDA21030400), DICP&QIBEBT UN201703.

■ REFERENCES

(1) Kholdeeva, O. A. Recent Developments in Liquid-phase Selective Oxidation Using Environmentally Benign Oxidants and Mesoporous Metal Silicates. *Catal. Sci. Technol.* **2014**, *4*, 1869−1889.
(2) Matsumoto, T.; Ueno, M.; Wang, N.; Kobayashi, S. Recent Advances in Immobilized Metal Catalysts for Environmentally Benign Oxidation of Alcohols. *Chem. - Asian J.* **2008**, *3*, 196−214.
(3) Guo, Z.; Liu, B.; Zhang, Q.; Deng, W.; Wang, Y.; Yang, Y. Recent Advances in Heterogeneous Selective Oxidation Catalysis for Sustainable Chemistry. *Chem. Soc. Rev.* **2014**, *43*, 3480−3524.
(4) Peng, H. G.; Xu, L.; Wu, H.; Zhang, K.; Wu, P. One-pot Synthesis of Benzamide over a Robust Tandem Catalyst Based on Center Radially Fibrous Silica Encapsulated TS-1. *Chem. Commun.* **2013**, *49*, 2709−2711.
(5) Li, P.; Cao, C.-Y.; Liu, H.; Yu, Y.; Song, W.-G. Synthesis of a Core-Shell-Shell Structured Acid-Base Bifunctional Mesoporous Silica Nanoreactor (MS-SO_3H@MS@MS-NH_2) and its Application in Tandem Catalysis. *J. Mater. Chem. A* **2013**, *1*, 12804−12810.
(6) Climent, M. J.; Corma, A.; Iborra, S. Heterogeneous Catalysts for the One-Pot Synthesis of Chemicals and Fine Chemicals. *Chem. Rev.* **2011**, *111*, 1072−1133.
(7) Kuwahara, Y.; Ando, T.; Kango, H.; Yamashita, H. Palladium Nanoparticles Encapsulated in Hollow Titanosilicate Spheres as an Ideal Nanoreactor for One-pot Oxidation. *Chem. - Eur. J.* **2017**, *23*, 380−389.
(8) Felpin, F. X.; Fouquet, E. Heterogeneous Multifunctional Catalysts for Tandem Processes: an Approach toward Sustainability. *ChemSusChem* **2008**, *1*, 718−724.
(9) Climent, M. J.; Corma, A.; Iborra, S. Mono- and Multisite Solid Catalysts in Cascade Reactions for Chemical Process Intensification. *ChemSusChem* **2009**, *2*, 500−506.
(10) Li, P.; Cao, C.-Y.; Chen, Z.; Liu, H.; Yu, Y.; Song, W.-G. Core-Shell Structured Mesoporous Silica as Acid-Base Bifunctional Catalyst with Designated Diffusion Path for Cascade Reaction Sequences. *Chem. Commun.* **2012**, *48*, 10541−10543.
(11) Yang, Y.; Liu, X.; Li, X.; Zhao, J.; Bai, S.; Liu, J.; Yang, Q. A Yolk-Shell Nanoreactor with a Basic Core and an Acidic Shell for Cascade Reactions. *Angew. Chem., Int. Ed.* **2012**, *51*, 9164−9168.
(12) Scotti, N.; Ravasio, N.; Zaccheria, F.; Psaro, R.; Evangelisti, C. Epoxidation of Alkenes through Oxygen Activation over a Bifunctional CuO/Al_2O_3 Catalyst. *Chem. Commun.* **2013**, *49*, 1957−1959.
(13) Luz, I.; León, A.; Boronat, M.; Llabrés i Xamena, F. X.; Corma, A. Selective Aerobic Oxidation of Activated Alkanes with MOFs and their Use for Epoxidation of Olefins with Oxygen in a Tandem Reaction. *Catal. Sci. Technol.* **2013**, *3*, 371−379.
(14) Aprile, C.; Corma, A.; Domine, M. E.; Garcia, H.; Mitchell, C. A Cascade Aerobic Epoxidation of Alkenes over Au/CeO_2 and Ti-mesoporous Material by "in situ" Formed Peroxides. *J. Catal.* **2009**, *264*, 44−53.
(15) Iwahama, T.; Hatta, G.; Sakaguchi, S.; Ishii, Y. Epoxidation of Alkenes Using Alkyl Hydroperoxides Generated in Situ by Catalytic Autoxidation of Hydrocarbons with Dioxygen. *Chem. Commun.* **2000**, 163−164.
(16) Peng, H.; Xu, L.; Zhang, L.; Zhang, K.; Liu, Y.; Wu, H.; Wu, P. Synthesis of Core−Shell Structured TS-1@Mesocarbon Materials and their Applications as a Tandem Catalyst. *J. Mater. Chem.* **2012**, *22*, 14219−14227.
(17) Remias, J. E.; Sen, A. Palladium-Mediated Aerobic Oxidation of Organic Substrates: the Role of Metal versus Hydrogen Peroxide. *J. Mol. Catal. A: Chem.* **2002**, *189*, 33−38.
(18) Sundararaman, R.; Ma, X.; Song, C. Oxidative Desulfurization of Jet and Diesel Fuels Using Hydroperoxide Generated in Situ by Catalytic Air Oxidation. *Ind. Eng. Chem. Res.* **2010**, *49*, 5561−5568.
(19) Okada, S.; Ikurumi, S.; Kamegawa, T.; Mori, K.; Yamashita, H. Structural Design of Pd/SiO_2@Ti-Containing Mesoporous Silica Core−Shell Catalyst for Efficient One-Pot Oxidation Using in Situ Produced H_2O_2. *J. Phys. Chem. C* **2012**, *116*, 14360−14367.
(20) Okada, S.; Mori, K.; Kamegawa, T.; Che, M.; Yamashita, H. Active Site Design in a Core-Shell Nanostructured Catalyst for a One-Pot Oxidation Reaction. *Chem. - Eur. J.* **2011**, *17*, 9047−9051.
(21) Ikurumi, S.; Okada, S.; Nakatsuka, K.; Kamegawa, T.; Mori, K.; Yamashita, H. Enhanced Activity and Selectivity in the One-Pot Hydroxylation of Phenol by Pd/SiO_2@Fe-Containing Mesoporous Silica Core−Shell Catalyst. *J. Phys. Chem. C* **2014**, *118*, 575−581.
(22) Tsuji, J.; Shinohara, K. Process for Producing Propylene Oxide. U.S. Patent US6,646,139, 2003.
(23) Tsuji, J.; Shinohara, K. Process for Producing Propylene Oxide. U.S. Patent US8,481,764, 2013.
(24) Sun, Z.; Xu, J.; Du, Z.; Zhang, W. Decomposition of Cyclohexyl Hydroperoxide over Transition Metal-Free Zeolite H-beta. *Appl. Catal., A* **2007**, *323*, 119−125.
(25) Wang, M.; Ma, J.; Chen, C.; Zheng, X.; Du, Z.; Xu, J. Preparation of Self-Assembled Cobalt Hydroxide Nanoflowers and the Catalytic Decomposition of Cyclohexyl Hydroperoxide. *J. Mater. Chem.* **2011**, *21*, 12609−12612.
(26) Zheng, X.; Wang, M.; Sun, Z.; Chen, C.; Ma, J.; Xu, J. Preparation of Copper (II) Ion-Containing Bisimidazolium Ionic Liquid Bridged Periodic Mesoporous Organosilica and the Catalytic Decomposition of Cyclohexyl Hydroperoxide. *Catal. Commun.* **2012**, *29*, 149−152.
(27) Spier, E.; Neuenschwander, U.; Hermans, I. Insights into the Cobalt(II)-Catalyzed Decomposition of Peroxide. *Angew. Chem., Int. Ed.* **2013**, *52*, 1581−1585.
(28) Liu, M.; Shi, S.; Zhao, L.; Wang, M.; Zhu, G.; Zheng, X.; Gao, J.; Xu, J. Effective Utilization of in Situ Generated Hydroperoxide by a Co−SiO_2@Ti−Si Core−Shell Catalyst in the Oxidation Reactions. *ACS Catal.* **2018**, *8*, 683−691.
(29) Zhu, Z.; Xu, H.; Jiang, J.; Wu, H.; Wu, P. Hydrophobic Nanosized All-Silica Beta Zeolite: Efficient Synthesis and Adsorption Application. *ACS Appl. Mater. Interfaces* **2017**, *9*, 27273−27283.
(30) Li, R.; Xue, T.; Bingre, R.; Gao, Y.; Louis, B.; Wang, Q. Microporous Zeolite@Vertically Aligned Mg-Al Layered Double Hydroxide Core@Shell Structures with Improved Hydrophobicity and Toluene Adsorption Capacity under Wet Conditions. *ACS Appl. Mater. Interfaces* **2018**, *10*, 34834−34839.
(31) Wang, L.; Xiao, F.-S. The Importance of Catalyst Wettability. *ChemCatChem* **2014**, *6*, 3048−3052.
(32) Wang, M.; Wang, F.; Ma, J.; Chen, C.; Shi, S.; Xu, J. Insights into Support Wettability in Tuning Catalytic Performance in the Oxidation of Aliphatic Alcohols to Acids. *Chem. Commun.* **2013**, *49*, 6623−6625.
(33) Chen, X.; Qian, P.; Zhang, T.; Xu, Z.; Fang, C.; Xu, X.; Chen, W.; Wu, P.; Shen, Y.; Li, S.; Wu, J.; Zheng, B.; Zhang, W.; Huo, F. Catalyst Surfaces with Tunable Hydrophilicity and Hydrophobicity: Metal-organic Frameworks toward Controllable Catalytic Selectivity. *Chem. Commun.* **2018**, *54*, 3936−3939.
(34) Fu, L.; Li, S.; Han, Z.; Liu, H.; yang, H. Tuning the Wettability of Mesoporous Silica for Enhancing the Catalysis Efficiency of Aqueous Reactions. *Chem. Commun.* **2014**, *50*, 10045−10048.
(35) Hao, Y.; Jiao, X.; Zou, H.; Yang, H.; Liu, J. Growing a Hydrophilic Nanoporous Shell on a Hydrophobic Catalyst Interface for Aqueous Reactions with High Reaction Efficiency and in Situ Catalyst Recycling. *J. Mater. Chem. A* **2017**, *5*, 16162−16170.
(36) Shi, S.; Wang, M.; Chen, C.; Lu, F.; Zheng, X.; Gao, J.; Xu, J. Preparation of Hydrophobic Hollow Silica Nanospheres with Porous Shells and their Application in Pollutant Removal. *RSC Adv* **2013**, *3*, 1158−1164.
(37) Wang, L.; Sun, J.; Meng, X.; Zhang, W.; Zhang, J.; Pan, S.; Shen, Z.; Xiao, F.-S. A Significant Enhancement of Catalytic Activities

DOI: 10.1021/acsami.8b19704
ACS Appl. Mater. Interfaces 2019, 11, 14702−14712

in Oxidation with H_2O_2 over the TS-1 Zeolite by Adjusting the Catalyst Wettability. *Chem. Commun.* **2014**, *50*, 2012−2014.
(38) Wang, L.; Wang, H.; Liu, F.; Zheng, A.; Zhang, J.; Sun, Q.; Lewis, J. P.; Zhu, L.; Meng, X.; Xiao, F.-S. Selective Catalytic Production of 5-Hydroxymethylfurfural from Glucose by Adjusting Catalyst Wettability. *ChemSusChem* **2014**, *7*, 402−406.
(39) Chen, C.; Shi, S.; Wang, M.; Ma, H.; Zhou, L.; Xu, J. Superhydrophobic SiO_2-Based Nanocomposite Modified with Organic Groups as Catalyst for Selective Oxidation of Ethylbenzene. *J. Mater. Chem. A* **2014**, *2*, 8126−8134.
(40) Chen, C.; Xu, J.; Zhang, Q.; Ma, Y.; Zhou, L.; Wang, M. Superhydrophobic Materials as Efficient Catalysts for Hydrocarbon Selective Oxidation. *Chem. Commun.* **2011**, *47*, 1336−1338.
(41) Karimi, B.; Khorasani, M. Selectivity Adjustment of SBA-15 Based Tungstate Catalyst in Oxidation of Sulfides by Incorporating a Hydrophobic Organic Group inside the Mesochannels. *ACS Catal.* **2013**, *3*, 1657−1664.
(42) Nakatsuka, K.; Mori, K.; Okada, S.; Ikurumi, S.; Kamegawa, T.; Yamashita, H. Hydrophobic Modification of Pd/SiO_2@Single-Site Mesoporous Silicas by Triethoxyfluorosilane: Enhanced Catalytic Activity and Selectivity for One-pot Oxidation. *Chem. - Eur. J.* **2014**, *20*, 8348−8354.
(43) Carrado, K. A.; Xu, L.; Csencsits, R.; Muntean, J. V. Use of Organo- and Alkoxysilanes in the Synthesis of Grafted and Pristine Clays. *Chem. Mater.* **2001**, *13*, 3766−3773.
(44) Barmatova, M. V.; Ivanchikova, I. D.; Kholdeeva, O. A.; Shmakov, A. N.; Zaikovskii, V. I.; Mel'gunov, M. S. Titanium-Doped Solid Core-Mesoporous Shell Silica Particles: Synthesis and Catalytic Properties in Selective Oxidation Reactions. *Catal. Lett.* **2009**, *127*, 75−82.
(45) Fraile, J. M.; García, N.; Mayoral, J. A.; Santomauro, F. G.; Guidotti, M. Multifunctional Catalysis Promoted by Solvent Effects: Ti-MCM41 for a One-Pot, Four-Step, Epoxidation−Rearrangement−Oxidation−Decarboxylation Reaction Sequence on Stilbenes and Styrenes. *ACS Catal.* **2015**, *5*, 3552−3561.
(46) Feng, X.; Sheng, N.; Liu, Y.; Chen, X.; Chen, D.; Yang, C.; Zhou, X. Simultaneously Enhanced Stability and Selectivity for Propene Epoxidation with H_2 and O_2 on Au Catalysts Supported on Nano-Crystalline Mesoporous TS-1. *ACS Catal.* **2017**, *7*, 2668−2675.
(47) Jappar, N.; Xia, Q.; Tatsumi, T. Oxidation Activity of Ti-Beta Synthesized by a Dry-Gel Conversion Method. *J. Catal.* **1998**, *180*, 132−141.
(48) Marchese, L.; Gianotti, E.; Dellarocca, V.; Maschmeyer, T.; Rey, F.; Coluccia, S.; Thomase, J. M. Structure−Functionality Relationships of Grafted Ti-MCM41 Silicas Spectroscopic and Catalytic Studies. *Phys. Chem. Chem. Phys.* **1999**, *1*, 585−592.
(49) Sudhakar Reddy, J.; Sayari, A. A Simple Method for the Preparation of Active Ti Beta Zeolite Catalysts. *Stud. Surf. Sci. Catal.* **1995**, *94*, 309−316.
(50) Hasegawa, Y.; Ayame, A. Investigation of Oxidation States of Titanium in Titanium Silicalite-1 by X-ray Photoelectron Spectroscopy. *Catal. Today* **2001**, *71*, 177−187.
(51) Lim, S.; Ciuparu, D.; Pak, C.; Dobek, F.; Chen, Y.; Harding, D.; Pfefferle, L.; Haller, G. Synthesis and Characterization of Highly Ordered Co-MCM-41 for Production of Aligned Single Walled Carbon Nanotubes (SWNT). *J. Phys. Chem. B* **2003**, *107*, 11048−11056.
(52) Katsoulidis, A. P.; Petrakis, D. E.; Armatas, G. S.; Trikalitis, P. N.; Pomonis, P. J. Ordered Mesoporous CoO_x/MCM-41 Materials Exhibiting Long-range Self-organized Nanostructured Morphology. *Microporous Mesoporous Mater.* **2006**, *92*, 71−80.
(53) Hermans, I.; Peeters, J.; Jacobs, P. A. Autoxidation of Ethylbenzene: The Mechanism Elucidate. *J. Org. Chem.* **2007**, *72*, 3057−3064.
(54) West, Z. J.; Zabarnick, S.; Striebich, R. C. Determination of Hydroperoxides in Jet Fuel via Reaction with Triphenylphosphine. *Ind. Eng. Chem. Res.* **2005**, *44*, 3377−3383.

DOI: 10.1021/acsami.8b19704
ACS Appl. Mater. Interfaces 2019, 11, 14702−14712